



## The ultrastructure of nematocysts from the fishing tentacle of the Hawaiian bluebottle, *Physalia utriculus* (Cnidaria, Hydrozoa, Siphonophora)

Angel A. Yanagihara\*, Janelle M.Y. Kuroiwa, Louise M. Oliver & Dennis D. Kunkel  
Békésy Laboratory of Neurobiology, Pacific Biomedical Research Center, University of Hawaii at Manoa, 1993  
East West Road, Honolulu, Hawaii 96822; Corresponding author. Tel.: +1-808-956-8328; fax:  
+1-808-956-6984; E-mail: angel@pbrc.hawaii.edu

**Key words:** *Physalia utriculus*, bluebottle, nematocyst, cnidaria, cnidome, anisorhiza

### Abstract

Fishing tentacle nematocysts of the hydrozoan, *Physalia utriculus*, from Hawaiian coastal waters, were examined by light microscopy, as well as by scanning and transmission electron microscopy (SEM and TEM). Hawaiian *P. utriculus* has been assumed to be conspecific with the Australian morph based on general macroscopic descriptions. Ultrastructural examination using SEM and TEM revealed that the cnidome was composed of two sizes of heterotrichous anisorhizas as well as rare rhopaloids (less than one observed per 1,000 nematocysts). Beyond classification of the cnidome of Hawaiian *P. utriculus*, an unprecedented morphological structure was observed. Specifically, SEM revealed fibers ( $< 1 \mu\text{m}$  in diameter) along the spiral crest of spines of some discharged tubules of *P. utriculus* anisorhizas. A hypothetical model of spine morphogenesis was formulated based on comparative analysis of hundreds of discharged tubules.

### Introduction

*Physalia utriculus* (La Martinière), a float-bearing siphonophore, amass and beach in large numbers along windward (eastern) Hawaiian shores following episodes of strong trade winds. A corresponding increase in human envenomations usually occurs as a result, with up to 500 stings per month recorded along the North Shore and Windward coasts (Thomas & Scott, 1997). Mature *P. utriculus* typically exhibit a clear to bluish-colored pneumatophore (float), up to 50 mm in length, and one predominant fishing tentacle of up to 1 m in length (Fenner et al., 1996). In contrast, the larger, carmine-crested Portuguese man-of-war, *Physalia physalis* (Linnaeus), which is common in Atlantic waters, as well as some Indo-Pacific zones is multi-tentaculate with fishing tentacles up to 30 m in length (Totton & Mackie, 1960; Halstead, 1988; Williamson et al., 1996). This distinction aside, *Physalia* spp. share the following anatomical features. Attached to the pneumatophore are gastrozooids, dactylozooids and reproductive gonophores

(Williamson et al., 1996). Dactylozooids of mature *P. utriculus* found in Hawaiian waters possess a single, long fishing tentacle, typically 1 m in length (Thomas & Scott, 1997). This cosmopolitan species is often confused with *P. physalis* which is rarely reported in Hawaiian coastal waters (Thomas & Scott, 1997) and was not observed during collections over the course of this four-year study. Although most researchers agree with the current classification of these two animals, they are very closely related and there is still some debate as to whether they should be considered conspecific (Williamson et al., 1996). The elucidation of cnidomes for each species may assist in solving this contentious issue.

Hydrozoans, like other cnidarians contain numerous stinging subcellular organelles, called cnidae, used primarily for prey capture and defense (Weill, 1934; Hyman, 1940; Yanagita & Wada, 1959; Mariscal, 1974a; Rifkin & Endean, 1983; Blanquet, 1988; Watson, 1988). The diversity of cnidae across the phylum has directed the development of standardized terminology (Watson & Wood, 1988) and a classific-

Table 1. Capsule sizes of heterotrichous anisorhizas from the fishing tentacle of *P. utriculus*

Nematocyst type	Mean						
	Capsule size at tentacle base $\mu\text{m}$	%	Capsule size at mid tentacle $\mu\text{m}$	%	Capsule size at tentacle tip $\mu\text{m}$	%	Capsule size $\mu\text{m}$
Small Anisorhiza	11.30 $\pm$ 2.4	43	10.85 $\pm$ 0.6	46	12.16 $\pm$ 0.6	53	11.0
Large Anisorhiza	21.87 $\pm$ 4.1	57	25.73 $\pm$ 0.9	54	27.19 $\pm$ 1.6	47	25.0

N values are 5  $\pm$  standard deviation

ation scheme based on both morphology and function (Weill, 1934; Southcott, 1956; Mariscal, 1974b; Williamson et al., 1996). Thus far, all cnidae observed in siphonophore fishing tentacles are of the nematocyst type (versus spirocysts, ptychocysts). There have been differences in the reported cnidome composition of *P. physalis*. The detailed study of Totton and Mackie of *P. physalis* reported large and small holotrichous isorhizas along the tentacles, small isorhizas along the gastrozoid lip-region and stenoteles in its gastrozoids and dactylozoids palpons and float (Totton & Mackie, 1960). However, the cnidome of *P. physalis* has also been variously identified as: atrichous isorhizas (Weill, 1934); two sizes of spherical isorhizas (Purcell, 1984); two sizes of holotrichous isorhizas (Hulet et al., 1974); euryteles and anisorhizas (Klug et al., 1988); and isorhizas and euryteles (Weber, 1991).

Accurate identification of the cnidome is essential in the analysis of venoms and understanding the potential plasticity of predator-prey relationships. Specifically, cnidarian venoms not only vary in composition between species, but also between nematocyst types within a species (Edean & Rifkin, 1975; Burnett et al., 1986; Hessinger, 1988). Cnidarian venoms consist of an array of biologically active compounds (Baxter & Marr, 1969; Crone & Keen, 1970; Auerbach & Taylor Hays, 1987; Halstead, 1988; Burnett, 1992; Bloom et al., 1998; Chung et al., 2001). The two sizes of *P. physalis* nematocysts have some differential toxicity (Burnett et al., 1986). Similarly, Klug and colleagues (1988) observed hemolytic activity of *P. physalis* euryteles discharged onto red blood cell smear slides while the anisorhizas discharge failed to elicit hemolysis.

Similarly, despite the lack of elucidation of the cnidome of *P. utriculus*, toxinological studies demonstrate that the venom that exhibits various biological

activity (lethal, hemolytic, hemorrhagic, neurotoxic) (Alam & Qasim, 1991, 1992, 1996). Indeed, there appears to have been little research performed on *P. utriculus* nematocysts, except for basic light microscopy on the Australian morph (Williamson et al., 1996) which we have assumed to be the same species. Rifkin identified the nematocysts of the Australian Pacific *P. utriculus* as isorhizas (Williamson et al., 1996). In this study, we investigated the ultrastructural characteristics of the nematocysts from locally captured *P. utriculus*, which are identified based on their small size and single long fishing tentacle (cf. *P. physalis*). With the aid of electron microscopy, we set out to fully characterize the fishing tentacle nematocysts.

## Materials and methods

### Specimen collection

*P. utriculus* were caught on northeast-facing shores (windward Oahu, Hawaii) during periods of on-shore winds above 10 km/h. Specimens were typically small, with pneumatophore lengths of 10 to 50 mm. *P. utriculus* were kept in sea water for up to 4 h, before having their fishing tentacle excised or being placed in mgCl<sub>2</sub> prior to fixation for scanning electron microscopy (SEM).

### Nematocyst isolation

Excised tentacles were kept in cold (4°C) seawater and spontaneously "shed" nematocysts were harvested at 24 h intervals for up to 7 days. Specifically, each morning, the tentacles and seawater were filtered using a 0.5 mm mesh sieve; the filtrate was then centrifuged (10 min at 3000 $\times$  g) to obtain a nematocyst pellet.

### Light microscopy

Tentacles from live animals were freshly excised on ice and placed in filtered sea water for observation by differential interference contrast microscopy (40–100 $\times$  magnification) with an inverted IX 70 Olympus microscope. Tentacle morphology and the morphology of *in situ* nematocysts were observed.

### Scanning electron microscopy (SEM)

Freshly caught *P. utriculus* were immediately placed in 7.5%  $\text{mgCl}_2$  for 15 min to cause tentacle relaxation. Thereafter, the animals were placed in distilled water for 1–2 min to induce nematocyst discharge. Alternatively, tentacles were stimulated to discharge their nematocysts by gently manipulating them with a rubber glove. Tentacles were excised and placed in a fixative, containing 2% glutaraldehyde in 0.1 m phosphate buffered saline, (PBS), pH 7.4 and 0.2 m sucrose for 18–24 h at 4°C. All tissue samples were postfixed in 1% osmium tetroxide ( $\text{OsO}_4$ ) in 0.1 m sodium cacodylate buffer for 1 h. Following rinses in the same buffer (30 min total), the sections were dehydrated in an ascending ethanol series from 10% to 100%, critical point dried using liquid  $\text{CO}_2$  (Tousimis Critical Point Dryer), mounted and metal coated (Hummer Sputter Coater II). Samples were examined using a Hitachi S-800 field emission scanning electron microscope.

### Transmission electron microscopy (TEM)

Isolated nematocysts were fixed in 1.5–2.0% glutaraldehyde in 0.1 m PBS for 18 h. Thereafter, nematocysts were rinsed in 0.1 m sodium cacodylate buffer for 30 min then postfixed in 1%  $\text{OsO}_4$  prepared in the same buffer for 60 min. Following rinses in the same buffer (30 min total), fixed nematocysts were dehydrated in ethanol and embedded in Spurr's epoxy resin. Thin sections were cut and examined unstained or stained (uranyl acetate and lead citrate) using a LEO 912 EFPM transmission electron microscope.

### Statistical analysis

Capsule sizes and tubule measurements were compared using the one-tailed students *t*-test.

## Results

### Fishing tentacle and *in situ* nematocyst morphology

Light microscopic examination of fresh tentacles of *P. utriculus* revealed (Figs. 1A, 1A inset i, and 1B) small (Fig. 1B, arrowheads) and large (Fig. 1B, arrows) nematocysts, (broadly described as haplonemes based on initial light microscopic examination and more specifically categorized as heterotrichous anisorhizas by detailed electron microscopic measurements that evidenced tubule tapering, as will be described below). A densely coiled tubule was apparent within the capsules (Fig. 1B). The tubule diameter was resolved in discharged isolated haplonemes and lacked any dramatic distension at the base (Fig. 1B, inset).

These nematocysts were densely packed in a relatively ordered arrangement (Fig. 1A, inset), and exhibited surface fibrils ( $\sim 200$  nm diameter and 800 nm length) (Fig. 1D). The percentage of large nematocysts appeared to decrease slightly from the tentacle base (Fig. 1A, inset) towards the tip of the tentacle (Fig. 1B), while the size of both nematocyst types appeared to increase concomitantly (Table 1).

The morphological characteristics of tentacles and nematocysts were examined using SEM. The tentacles of *P. utriculus*, were quite distinct from those of other jellyfish, in that nematocysts were located on only one side of the tentacle (Fig. 1C), opposite to the muscular aspect (Fig. 1C, arrow) of the tentacle. Under higher magnification, round, convex-surfaced nematocysts appeared packed with each possessing a small projection in the center (Fig. 1D, arrows) in the midst of projection-lacking irregular-shape bordered cells.

Large nematocysts found in the fishing tentacle were approximately 25  $\mu\text{m}$  ( $\pm$  SE 2.08) in diameter (Fig. 1B, arrows). Smaller nematocysts measured approximately 11  $\mu\text{m}$  ( $\pm$  SE 0.35) in diameter (Fig. 1B, arrowheads). Nematocysts located at the base of the fishing tentacle appear to be slightly smaller than those at the tentacle tip (Table 1). While these values showed a gradient of larger nematocyst size from tentacle base to tip, sizes were not statistically different within the data set analyzed by the student's *t* test ( $p > 0.05$ ).

SEM of discharged nematocysts revealed the opercula to be circular, 3  $\mu\text{m}$  in diameter and 2  $\mu\text{m}$  in apparent depth (Fig. 2A, arrow). A longitudinal section TEM of an undischarged nematocyst clearly showed the "plug-like" nature of this structure at the apex of the capsule (Fig. 2D).

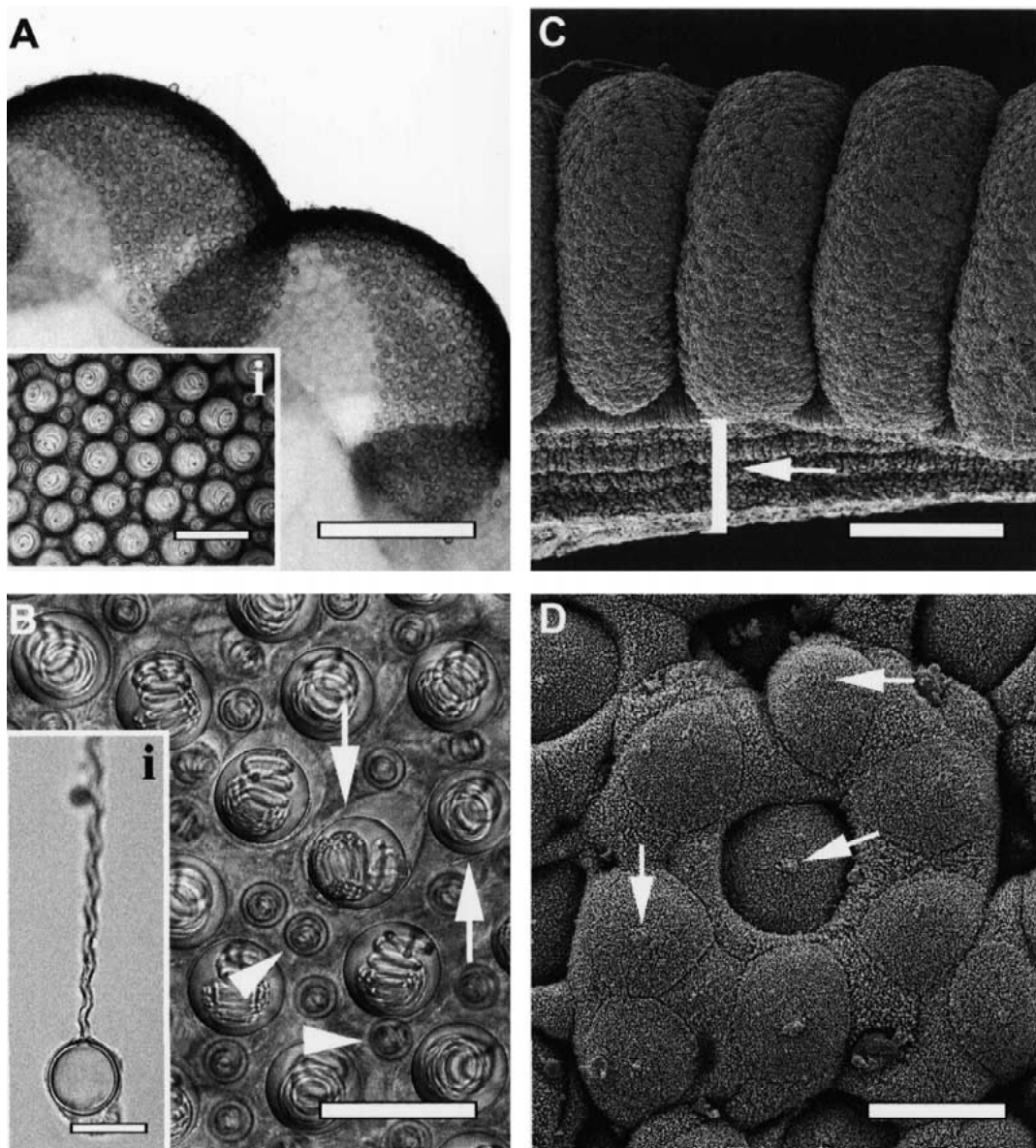


**Figure 1.** LM and SEM of *P. utriculus* fishing tentacles and heterotrichous anisorhizas. (A) LM of contracted fishing tentacle of *P. utriculus*, mid to tip region. Note the distinct nematocyst containing bulges producing the ridged appearance of tentacle. Nematocysts are visible as spherical white spots through the tentacle tissue. Bar: 300  $\mu\text{m}$ . A higher magnification shows the orderly arrangement of nematocysts near the base of the tentacle (inset). This image also indicates nematocysts separated in different planes, the larger anisorhizas appear to be set deeper in the tentacle tissue. Bar: 50  $\mu\text{m}$ . (B) Higher magnification LM of *in situ* undischarged nematocysts. Two sizes of anisorhizas are observed, small (arrowhead) and large (arrow). Tightly coiled tubules are visible within the undischarged capsules. Bar: 40  $\mu\text{m}$ . A large isolated discharged anisorhiza on acrylamide gel is shown (inset). Note empty capsule and spiral-like appearance of tubule. Bar: 25  $\mu\text{m}$ . (C) Low magnification SEM of a contracted fishing tentacle. Note the muscular aspect of the tentacle (arrow) devoid of nematocysts. Nematocysts are located on only one side of the tentacle opposite this muscle band, in button-like (beaded?) ridges. Bar: 300  $\mu\text{m}$ . (D) SEM of tentacle surface with packed nematocysts covered by a distinct epithelial layer. The epithelial surface possesses small papillae and cnidocils (arrows). Nematocysts appear to exist *in situ* in a rosette-like pattern when viewed by SEM. Bar: 15  $\mu\text{m}$ .

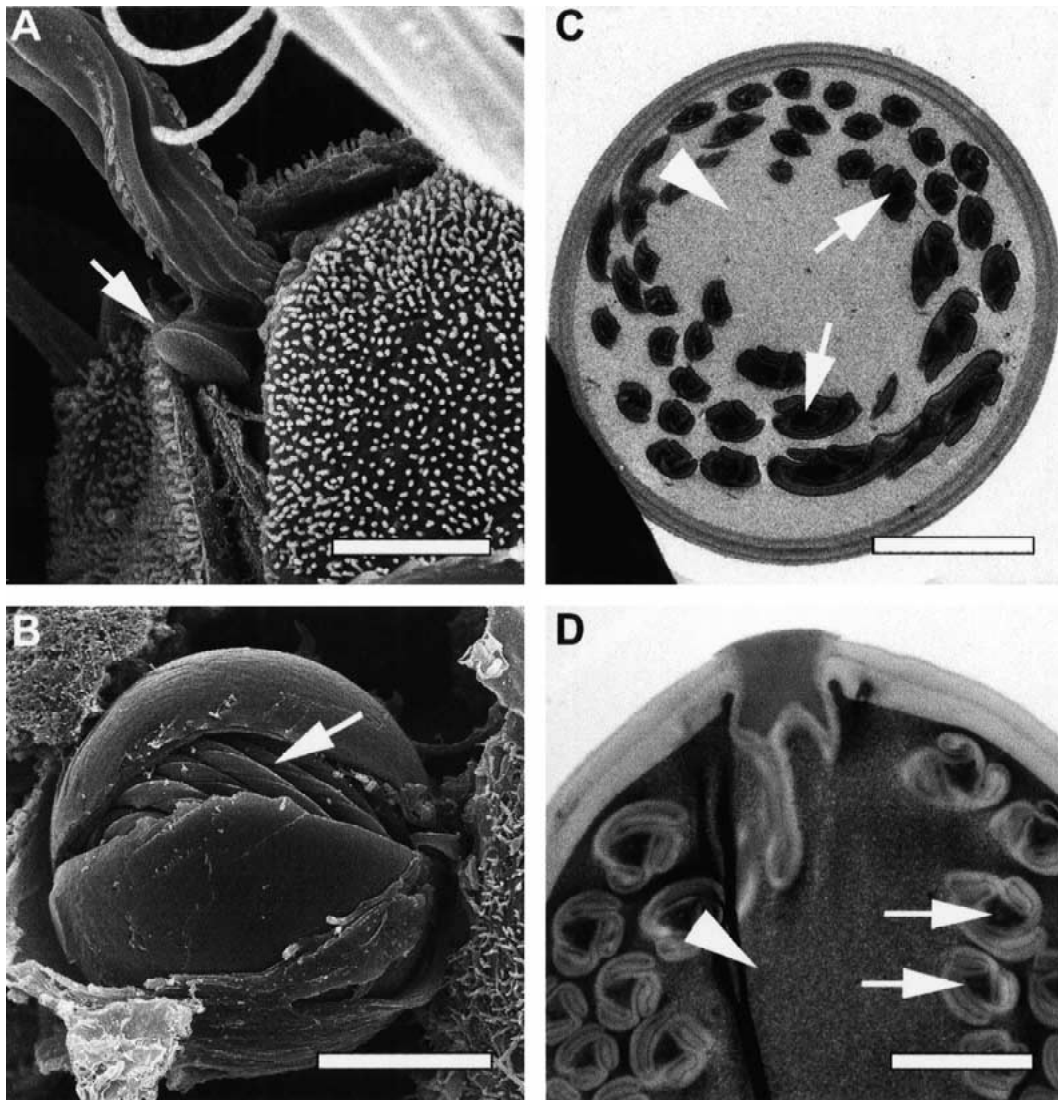


**Figure 2.** SEM and TEM of discharged, fractured and undischarged *P. utriculus* heterotrichous anisorhizas. (A) Large *in situ* discharged heterotrichous anisorhiza showing circular-shaped, plug-like operculum (arrow). Bar: 5  $\mu\text{m}$ . (B) Fractured nematocyst capsule demonstrating the tightly coiled smooth nature of the pre-everted tubule (arrow). Bar: 10  $\mu\text{m}$ . (C) TEM longitudinal section of heterotrichous anisorhiza capsule showing the pre-everted tubules with both electron-dense and electron-lucent material observable in the core (arrows). The capsule matrix is electron-dense (arrowhead). Note the opercular cap at the apex of the capsule. Bar: 4  $\mu\text{m}$ . (D) TEM transverse section of heterotrichous anisorhiza capsule showing the pre-everted tubules around the periphery with electron dense cores (arrows). The capsule matrix is electron-lucent (arrowhead). Note the lack of a central shaft. Bar: 8  $\mu\text{m}$ .

#### *Undischarged nematocyst morphology*

Some nematocysts fractured during simple preparations involving rapid dehydration. Such split capsules provided structural information on the morphology of the tubules in their pre-everted state. Pre-everted tubules from a fractured capsule (Fig. 2B) appeared

twisted and smooth, in contrast to discharged (everted) tubules which exhibited prominent spines (Figs. 3B-D). In addition, analysis of TEM transverse and longitudinal sections revealed electron-dense spines within gradually tapering tubule sections in an outside-in orientation and the lack of a large diameter tubule base or shaft (cf. heteronemes) (Figs. 2C and 2D).

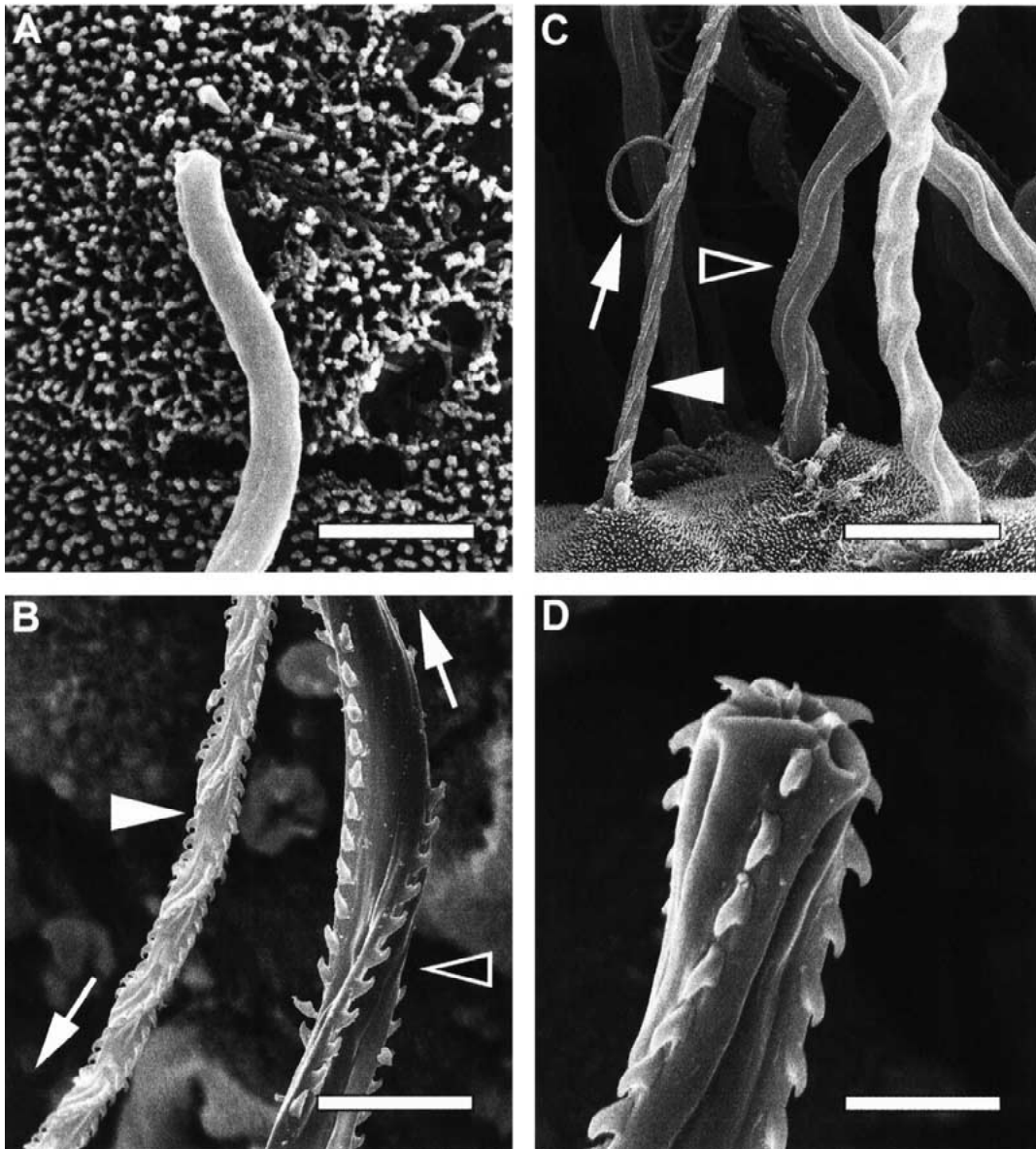


Figure 3. SEM of discharged *P. utriculus* heterotrichous anisorhiza tubules. (A) SEM of spineless tip of large heterotrichous anisorhiza tubule. Bar: 3  $\mu\text{m}$ . (B) SEM of mid-tubule region of heterotrichous anisorhizas. A small diameter tubule (solid arrowhead) and a large diameter tubule (open arrowhead) contain numerous claw-shaped spines. Each spine along the crest is angled downward; the arrows point towards the capsules, indicating the direction of spines is identical for both sizes of heterotrichous anisorhizas. Bar: 6  $\mu\text{m}$ . (C) SEM of proximal tubules of heterotrichous anisorhizas. Small diameter (solid arrowhead) and large diameter tubules (open arrowhead) are shown. The base region of the small tubule shows the coiled structure (arrow) around the tubule. Bar: 10  $\mu\text{m}$ . (D) High magnification SEM of spines on an everting large heterotrichous anisorhiza tubule. Bar: 3  $\mu\text{m}$ .

#### Tubule morphology

The tubules from the large and small nematocysts everted to a maximum length 660  $\mu\text{m}$  and 250  $\mu\text{m}$ , respectively (Table 2). The smaller nematocysts exhibited thin tubules with a mean diameter of 1.5  $\mu\text{m}$ ,

while the larger nematocysts exhibited tubules with a mean diameter of 3.3  $\mu\text{m}$  (Fig. 3B). Tubules of both nematocyst types decreased in diameter from base to tip. The tapering of the tubules was investigated in depth. The smaller nematocysts had a tubule tip diameter of 0.84  $\mu\text{m} \pm 0.2$  S.D., approximately half

Table 2. Tubule characteristics of heterotranchous anisorhizas from the fishing tentacle of *P. utriculus*.

Nematocyst type	Tubule section	Surface area per spine $\mu\text{m}^2$	Spines per 1 $\mu\text{m}$ length	Tubule diameter $\mu\text{m}$	Tubule length $\mu\text{m}$	Fiber width $\mu\text{m}$
Small Anisorhiza	Proximal	0.06	4	1.70±0.20		
	Mid-Distal	–	–	1.52± 0.36		
	Tip	No spines	No spines	0.84±0.20		
	<b>Total</b>				250±18	0.46±0.12
Large Anisorhiza	Proximal	0.08	3	3.80±0.44		
	Mid-Distal	–	–	3.34±0.62		
	Tip	No spines	No spines	2.5±0.52		
	<b>Total</b>				660 ±110	0.93±0.15

N values are 5 ± standard deviation.

that of the tubule base diameter ( $1.7 \mu\text{m} \pm 0.2$  S.D.). This difference was statistically significant (students *t* test,  $p=0.00007$ ). Similarly, the larger nematocysts had a tubule tip diameter of  $2.5 \mu\text{m} \pm 0.5$  S.D., approximately two-thirds of the tubule base diameter ( $3.8 \mu\text{m} \pm 0.4$  S.D.). This difference was also statistically significant (students *t*-test,  $p=0.001$ ). Based upon these measurements, the nematocysts were more specifically described as anisorhizas.

#### Spine morphology

Three rows of regular, cat-claw shaped spines were apparent on the tubules (Figs. 3B-D). This triple crest of spines was arranged spirally along the length of the tubules, until approximately  $10 \mu\text{m}$  from the tip. Both sizes of anisorhizas exhibited tubules with tapered tips devoid of spines (Fig. 3A). One case of arrested discharge was observed in which the tubule terminus was spine covered (Fig. 3D) as the tubule eversion was incomplete. The average surface area of spines was greater on the large anisorhizas, and there was a gradual decrease in spine size from mid-length until the point where the tubules exhibited no spines in both types (Table 2). Based upon these features, these anisorhizas were more specifically described as heterotranchous anisorhizas.

#### Fiber morphology

A coiled fibrous structure was commonly observed wrapped around the base of discharged heterotranchous anisorhiza tubules of both nematocyst sizes and also at times completely covering the tubule spines (Figs. 4A-D). The surface of this fiber had a scale-

like appearance (Fig. 4C, arrow) and the fiber width measured an average of  $0.72 \mu\text{m}$ . The fiber frequently extended along the complete length of the discharged tubule and in some nematocysts appeared to be either contiguous with or covering the spines (Fig. 4B and 4D, arrowhead). Analysis of SEM images indicated that the fiber varied in diameter between nematocysts. Small tubule fibers varied in width from  $0.32$ - $0.65 \mu\text{m}$ , and large fibers varied from  $0.83$ - $1.22 \mu\text{m}$  (Table 2). In some cases, the fibers appeared to have encased the spines and subsequently to have separated from the underlying spines in exhibiting corresponding recessed spine-sized grooves. In other cases, the fiber was lifted away from a section of the tubule which lacked spines. The large fibers were 0.31 times as wide as the large tubule, while the smaller fibers measured 0.24 times the width. The surface appearance of the fiber and spines were comparable and differed markedly from the tubule and capsule external surfaces.

#### Discussion

While the literature contains a number of careful studies reporting about the cnidome and venom of *P. physalis*, few studies have investigated *P. utriculus*. This study was undertaken to elucidate the morphology and venom composition of the nematocysts in the fishing tentacles of the hydrozoan species responsible for the highest number of jellyfish stings in Hawaiian waters. *P. utriculus*, present in significant numbers throughout the year, can inflict serious envenomations that cause immediate, long-term or delayed allergic reactions (Thomas & Scott, 1997). At present, it has not been determined which specific nematocyst types

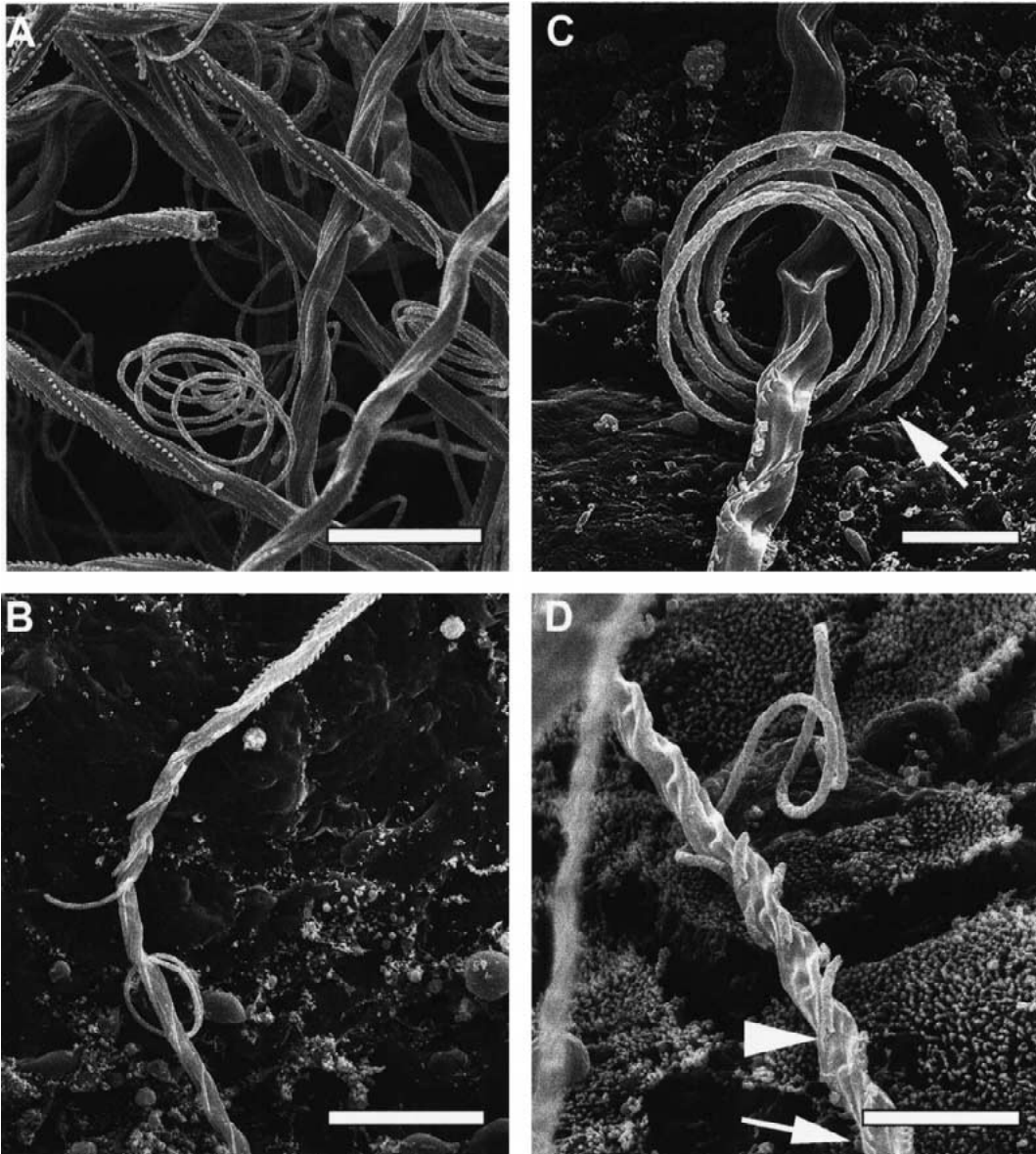


**Figure 4.** SEM of “fiber-like” structures of *P. utriculus* heterotrichous anisorhizas. (A) SEM showing fibers and matted tubules of large discharged heterotrichous anisorhizas. Bar: 20  $\mu\text{m}$ . (B) SEM of single heterotrichous anisorhiza tubule. Note the presence of spines toward the tip and the sloughing off of this crest towards the proximal tubule. A section of fiber is coiled around the proximal tubule. Bar: 12  $\mu\text{m}$ . (C) High magnification SEM of fiber coiled around the base of a large heterotrichous anisorhiza tubule. Note the segmented appearance of the fiber surface (arrow). Bar: 8  $\mu\text{m}$ . (D) High magnification SEM of heterotrichous anisorhiza tubule generally lacking spines except towards the tip (arrow). Note the segmented appearance of the fiber and the contiguous nature with the spine crest (arrowhead). Bar: 6  $\mu\text{m}$ .

in *P. utriculus* is responsible for the various effects of the venom.

#### *Cnidome*

The cnidome of the Hawaiian *P. utriculus* differed slightly from the previously described cnidome of *P.*

*utriculus* (Australian morph) and the closely related Atlantic Portuguese Man-o-War (*P. physalis*) which has also been documented with a cnidome paralleling the Australian *P. utriculus* species. The cnidae observed in *P. utriculus* are broadly classified as haplonemes (lacking a defined distended tubule base or shaft), and initially appeared comparable (using light

microscopy) to some published reports of the cnidome of the Australian *P. utriculus* (Cleland & Southcott, 1965; Williamson et al., 1996) and *P. physalis* (Lane & Dodge, 1958; Hulet et al., 1974; Hessinger & Ford, 1988). However, based on SEM evidence of tapering of the tubules in both small and large haplonemes, nematocysts in *P. utriculus* are identified as anisorhizas, not isorhizas as previously described (Cleland & Southcott, 1965; Williamson et al., 1996). The nematocyst keys currently published, such as that developed by Mariscal (1971) and revised in Williamson and colleagues (1996) do not specify exact dimensions, and utilize such non-specific definitions as "slight narrowing of the tubule" which are open to interpretation. As such, with the benefit of SEM we have taken accurate measurements of nematocyst tubules and arbitrarily interpreted tapering of more than 30% to be significant. This newly described Hawaiian *P. utriculus* cnidome is similar to that reported by Klug and colleagues (1988) for the closely related Atlantic *P. physalis* cnidome.

Furthermore, the anisorhizas may be reported as heterotrichous based on the changes in spine sizes along the tubules, in that, there is a decrease in spine size towards the distal end of the tubule immediately prior to the spineless tip. The spines do appear quite uniform in size along most of the proximal to mid-tubule length, consistent with the previous light microscopy based holotrichous classification. However, SEM evidence reveals the slight decrease in spine sizes; thus, applying the nematocyst key literally ("spines of unequal size") (Mariscal, 1971), these anisorhizas appear heterotrichous.

No nematocyst capsule sizes have been published for *P. utriculus*, but capsule sizes have been recorded for *P. physalis*. Lane & Dodge (1958) first reported the size of the capsules as 11.3  $\mu\text{m}$  and 26.8  $\mu\text{m}$ , very similar to Hulet et al. (1974), who reported measurements of 11.3  $\mu\text{m}$  and 25.3  $\mu\text{m}$ , respectively. More recently, Purcell (1984) measured the nematocysts as 12.5  $\mu\text{m}$  and 27.5  $\mu\text{m}$ , respectively, slightly larger than previous records, while Burnett and colleagues (1986) recorded 10.6  $\mu\text{m}$  and 23.5  $\mu\text{m}$ , somewhat smaller than initial reports. Our measurements for *P. utriculus* heterotrichous anisorhizas are comparable, lying within the ranges for both sizes of *P. physalis* nematocysts.

Heteronemes (nematocysts bearing well-defined shafts) have been reported in *P. physalis*, e.g. euryteles (Klug et al., 1988). While haplonemes (more precisely identified as heterotrichous anisorhizas) were

predominant, we did observe heteronemes in both whole tentacle and isolated shed nematocyst preparations, but they appeared to constitute less than 2% of the cnidome. These heteronemes were only observed using light microscopy, so we hesitate to further accurately classify these nematocysts. None of the heteronemes were observed in SEM images of fishing tentacle surfaces, which again suggests they may make up a very small percentage of the cnidome. Klug et al. (1988) reported a similar rarity for *P. physalis* euryteles, which interestingly exhibit significant hemolytic activity. Alam & Qasim (1996) reported hemolytic activity for *P. utriculus* nematocyst venom, but no details of nematocyst types were disclosed. Further investigations are required to determine if the heteroneme or haplonemes in *P. utriculus* are responsible for this activity. Another type of heteroneme, stenoteles, have been reported as present in the gastrozooids of *P. physalis* (Totton & Mackie, 1960), and although the primary focus of this study was to describe the nematocyst types in the fishing tentacles, we again observed similar nematocysts in the feeding tentacles of *P. utriculus*.

The change in undischarged nematocyst capsule sizes along the tentacle length is apparently not unique. The smaller capsule size at the base of the tentacle is probably indicative of immaturity. *P. physalis* produces nematocysts at this site, which then migrate down a central canal of the tentacle to their final position (Totton & Mackie, 1960). The ratio of the two sizes of nematocysts along the tentacle also varied. The decrease in the ratio of large anisorhizas from 57% at the tentacle base to 47% at the tentacle tip could be related to the decreasing area of the tentacle, but more probably reflects the loss of recently discharged nematocysts during prey capture.

#### *Nematocyst structures*

The circular opercula noted in both anisorhizas is perhaps of little significance for nematocyst classification purposes at least, as there does not appear to be any patterns established between opercula shape and nematocyst types thus far. A triangular operculum is documented in the euryteles of the cubozoan, *Chironex fleckeri* (Rifkin, 1987), while a circular operculum is noted in the isorhizas of the same species. The plug-like operculum (shape undefined) has been reported in *P. physalis* (Hessinger & Ford, 1988), but the opercula in *P. utriculus* have not been described previously. While we can report that *P. utriculus*

nematocysts have a circular plug-like operculum, we deduce that operculum shape appears to be neither species, class, nor nematocyst type specific.

Previous studies (Skaer & Picken, 1965; Skaer, 1973; Watson & Mariscal, 1984) report that nematocyst capsule matrix is usually electron dense and the capsule wall transparent in immature nematocysts (Fig. 2D, arrowhead), while the opposite occurs in mature nematocysts, i.e. translucent matrix and dense wall (Fig. 2C, arrowhead). Thus, the longitudinal TEM section of a *P. utriculus* heterotrichous anisorhiza may represent an immature nematocyst (Fig. 2D) while the TEM transverse section may represent a mature nematocyst (Fig. 2C). The electron-dense nature of the material within the pre-everted tubules of the TEM transverse section is also consistent with this interpretation. TEM images were somewhat inconclusive in showing the presence of the fiber in pre-everted tubules.

#### *Tubule fibers*

The coiled fiber on *P. utriculus* heterotrichous anisorhiza tubules has not been previously documented for any *Physalia* species, and indeed there appears to be no published pictorial (SEM) evidence of it observed in any discharged nematocysts of other species. While the possibility exists that it is a result of the fixation processes utilized during SEM, it could play a functional, but as yet undefined role. Blake et al. (1988) describe electron-lucent fibers in the grooves of the pleated inverted tubule of *Aiptasia pallida* (anthozoa) which they suggest may be involved in tubule maturation. Clausen (1991), in contrast, report electron-dense fibers within the tubule of *Halammohydra intermedia* (hydrozoa) nematocysts but make no suggestion as to their function.

Pending further research, we suggest a hypothesis for the function of the fiber. Our observation that *Physalia* sp. nematocysts can discharge even after fixation prompts us to consider that some fraction of discharged nematocysts are structurally immature but have discharged due to fixative conditions. It was evident that there was discharge primarily after the osmium fixation and to some further extent during the dehydration. This happened all of the time when osmium fixation was used after the aldehyde. Omitting the osmium fixation resulted in much less release but resulted in more problems with tissue-shrinkage and sample charging. If immature nematocysts are discharged, such may exhibit transient structures in-

volved in the morphogenesis of spines. Based on this morphological evidence alone, we suggest the hypothesis that the fiber is a precursor material from which the spines develop. Thus, the fiber may only be present during the developmental stage of the anisorhiza. This is supported by the observation that it appears to be found with tubules where spines are either lacking or immature. Additionally, the fiber appears to be absent on discharged nematocyst tubules exhibiting the full complement of large mature spines. Further, high concentrations of calcium have been recorded from fully mature nematocysts (Lubbock et al., 1981), with calcium transport into the nematocyst reportedly occurring after tubule inversion during the final maturation stage, i.e. spine formation (Skaer, 1973). Watson (1988) reports an accumulation of calcium-binding material along the tubule wall in mature *Physalia* nematocysts. We suggest that a calcification process occurs within the fiber to form the spines. Redundant material between the spines may then be hydrolyzed or resorbed, as no fiber remnants were observed. A schematic is presented below to illustrate this concept (Figure 5).

This interpretation of spine development on tubules differs slightly from that proposed by Skaer (1973). Possible explanations for this include the fact that species and nematocyst types differed, and furthermore, this study had the benefit of SEM. Spines are evidently the last structures to develop in nematocysts, thus, we cautiously suggest that the presence of the fiber may be indicative of undeveloped spines. It may therefore only be observable in immature anisorhiza nematocysts, which normally would not discharge under natural conditions. Further biochemical and developmental studies are warranted to validate the ultrastructural data and to ensure that the fiber is not some artifact resulting from our SEM processing.

#### **Acknowledgements**

We thank Drs. David Hessinger, Peter Anderson, Ian Cooke, Massimo Avian, Jamie Seymour, and Jesse Stolberg for thoughtful discussions and Ms. Tina Weatherby for technical assistance in embedding, sectioning and analyzing EM samples at the Biological Electron Microscope Facility, which is supported in part by grant G12RR03061 from the Research Centers in Minority Institutions Program of the National Center for Research Resources, National Institutes of Health. This work was supported by grants from the

Victoria and Bradley Geist Foundation (Hawaii Community Foundation), the Cades Fund, the University of Hawaii Research Council, and the Specialized Neuroscience Research Program (1U54NS39406) of the National Institutes of Health.

## References

- Alam, J.M. & R. Qasim, 1991. Toxicology of *Physalia's* (Portuguese man-o'-war) venom. *Pakistan J. Pharmaceut. Sci.* 4: 159–168.
- Alam, J.M. & R. Qasim, 1992. Preliminary studies on the biological and hazardous marine toxins from Karachi coast: (1) biochemical and biological properties of *Physalia* venom. *Toxicon* 30: 532.
- Alam, J.M. & R. Qasim, 1996. Isolation and physiopharmacological properties of three high molecular weight lethal proteins from a coelenterate (*Physalia utriculus*) venom. *Pakistan J. Zool.* 28: 245–252.
- Arneson, A.C. & C.E. Cutress, 1976. Life history of *Carybdea alata* Reynaud, 1830 (Cubomedusae). In: Mackie G.O. (Ed.), *Coelenterate Ecology and Behaviour*. New York, Plenum Publishing, pp. 227–236.
- Auerbach P.S. & J. Taylor Hays, 1987. Erythema nodosum following a jellyfish sting. *J. Emerg. Med.* 5: 487–491.
- Baker, H., 1743. An attempt towards a natural history of the polype. In: Hessinger, D. A. & H. M. Lenhoff (Eds.) 1988, *The Biology of Nematocysts*. Academic Press, Inc., San Diego, pp. 1–19.
- Baxter, E.H. & A.G.M. Marr, 1969. Seawasp venom – lethal hemolytic and dermonecrotic properties. *Toxicon* 7: 195–210.
- Blake, A.S., R.S. Blanquet & G.B. Chapman, 1988. Fibrillar ultrastructure of the capsular wall and intracapsular space in developing nematocysts of *Aiptasia pallida* (Cnidaria: Anthozoa). *Trans. Am. Microsc. Soc.* 107: 217–231.
- Blanquet R.S., 1988. The chemistry of cnidae. In: Hessinger D.A. & H.A. Lenhoff (Eds.), *The Biology of Nematocysts*. Academic Press, Inc., San Diego, pp. 407–425.
- Bloom, D.A., J.W. Burnett & P. Alderslade, 1998. Partial purification of box jellyfish (*Chironex fleckeri*) nematocyst venom isolated at the beachside. *Toxicon* 36:1075–1085.
- Burnett, J.W., 1992. Immunological aspects of jellyfish envenomations. In: Gopalakrishnakone P. & C. K. Tan (Eds.), *Recent Advances in Toxinology Research*. Venom and Research Group, Singapore, pp. 333–349.
- Burnett, J.W. & G.J. Calton, 1977. The chemistry and toxicology of some venomous pelagic coelenterates. *Toxicol* 15: 177–196.
- Burnett, J.W. & W.D. Gable, 1989. A fatal jellyfish envenomation by Portuguese man-o'-war. *Toxicon* 27: 823–824.
- Burnett, J.W., J.V. Ordonez & G.J. Calton, 1986. Differential toxicity of *Physalia physalis* (Portuguese Man-of-War) nematocysts separated by flow cytometry. *Toxicon* 24: 514–518.
- Chung, J.J., L.A. Ratnapala, I.M. Cooke & A.A. Yanagihara, 2001. Partial purification and characterization of a hemolysin (CAH1) from Hawaiian box jellyfish (*Carybdea alata*) venom. *Toxicon* 39: 981–990.
- Clausen, C., 1991. Differentiation and ultrastructure of nematocysts in *Halammohydra intermedia* (Hydrozoa, Cnidaria). *Hydrobiologia* 216/217: 623–628.
- Cleland, J.B. & R.V. Southcott, 1965. Injuries to man from marine invertebrates in the Australian region. *Special Report Series* (No.12). National Health and Medical Research Council, Canberra, Australia: 1965.
- Crone, H.D. & T.E.B. Keen, 1970. Further studies on the biochemistry of the toxins of the sea wasp *Chironex fleckeri*. *Toxicon* 9: 145–151.
- Endean, R. & J.F. Rifkin, 1975. Isolation of different types of nematocysts from the cubomedusan *Chironex fleckeri*. *Toxicon* 13: 375–376.
- Endean, R., C. Duchemin, D. McColm & E. Hope Fraser, 1969. A study of the biological activity of toxic material derived from nematocysts of the cubomedusan *Chironex fleckeri*. *Toxicon* 6: 179–204.
- Fenner, P.J., P.F. Fitzpatrick, R.J. Hartwick & R. Skinner, 1985. "Morbakka", another cubomedusan. *Med. J. Aust.* 143: 550–555.
- Fenner, P.J., J. Rifkin & J.A. Williamson, 1996. *Physalia utriculus* (Bluebottle). In: Williamson, J. A., P. J. Fenner, J. W. Burnett, J. F. Rifkin (Eds), *Venomous and Poisonous Marine Animals. A Medical and Biological Handbook*. University of New South Wales Press, Sydney, Australia, pp. 200.
- Fenner, P.J. & J.A. Williamson, 1996. Worldwide deaths and severe envenomation from jellyfish stings. *Med. J. Aust.* 165: 658–661.
- Halstead, B.W., 1988. *Poisonous and venomous marine animals of the world* (2nd revised edition). Darwin Press, Princeton, NJ, 1168 pp.
- Hessinger, D.A., 1988. Nematocyst venoms and toxins. In: Hessinger, D. A. & H. M. Lenhoff (Eds.), *The Biology of Nematocysts*. Academic Press, Inc., San Diego, pp. 333–369.
- Hessinger, D.A. & M.T. Ford, 1988. Ultrastructure of the small cnidocyte of the Portuguese Man-of-War (*Physalia physalis*) tentacle. In: Hessinger, D. A. & H. M. Lenhoff (Eds.), *The Biology of Nematocysts*. Academic Press, Inc., San Diego, pp. 75–94.
- Hulet, W.H., J.L. Belleme, G. Musil & C.E. Lane, 1974. Ultrastructure of *Physalia* nematocysts. In: Humm H.J. & C.E. Lane (Eds.), *Bioactive Compounds from the Sea*. Marcel Dekker, New York, pp. 99–114.
- Hyman, L.H., 1940. *The invertebrates: Protozoa through Ctenophora*, Vol I. McGraw-Hill, New York, pp. 365–661.
- Kaplan, E.H., 1982. *A Field Guide to Coral Reefs of the Caribbean and Florida*. Houghton Mifflin Company, Boston.
- Klug, M., J. Weber & P. Tardent, 1988. Direct Observation of hemolytic activity associated with single nematocysts. In: Hessinger, D. A. & H. M. Lenhoff (Eds.), *The Biology of Nematocysts*. Academic Press, Inc., San Diego, pp. 543–550.
- Lane, C.E. & E. Dodge, 1958. The toxicity of *Physalia* nematocysts. *Biol. Bull.* 115: 219–226.
- Lubbock, R., B.L. Gupta & T.A. Hall, 1981. Novel role of calcium in exocytosis: Mechanism of nematocyst discharge as shown by X-ray microanalysis. *Proc. Natl. Acad. Sci. U.S.A.* 78: 3624–3628.
- Mariscal, R.N., 1971. Effect of a disulfide reducing agent on the nematocyst capsules from some coelenterates, with an illustrated key to nematocyst classification. In: Lenhoff, H.M., L. Muscatine & L.V. Davis (Eds.), *Experimental Coelenterate Biology*. University of Hawaii Press, Honolulu, pp. 157–168.
- Mariscal, R.N., 1974a. Scanning electron microscopy of the sensory surface of the tentacles of sea anemones and corals. *Z. Zellforsch. Mikrosk. Anat.* 147: 149–156.
- Mariscal, R.N., 1974b. Nematocysts. In: Muscatine, L. & H.M. Lenhoff (Eds.), *Coelenterate Biology: Reviews and new perspectives*. Academic Press, New York, pp. 129–178.

- Purcell, J.E., 1984. The functions of nematocysts in prey capture by epipelagic siphonophores (Coelenterata, Hydrozoa). *Biol. Bull.* 166: 310–327.
- Rifkin, J.F., 1987. Studies of the structure, arrangement and mode of operation of cnidae from cnidarians belonging to the classes cubozoa, hydrozoa, scyphozoa and anthozoa. Ph.D. Thesis. University of Queensland, Brisbane, Australia.
- Rifkin, J.F. & R. Endean, 1983. The structure and function of the nematocysts of *Chironex fleckeri* Southcott 1956. *Cell Tissue Res.* 233: 563–577.
- Skaer, R.J., 1973. The secretion and development of nematocysts in a siphonophore. *J. Cell. Sci.* 13: 371–393.
- Skaer, R.J. & L.E.R. Picken, 1965. The structure of the nematocyst thread and the geometry of discharge in *Corynactis viridis* Allman. *Phil. Trans. R. Soc. Ser. B.* 250: 131–164.
- Southcott, R.V., 1956. Studies on Australian cubomedusae, including a new genus and species apparently harmful to man. *Australian J. Marine Freshwater Res.* 7: 254–280.
- Southcott, R.V., 1967. Revision of some carybdeidae (Scyphozoa: Cubomedusae), including a description of the jellyfish responsible for the “Irukandji Syndrome”. *Aust. J. Zool.* 15:651–671.
- Tamkun, M.M. & D.A. Hessinger, 1981. Isolation and partial characterization of a hemolytic and toxic protein from the nematocyst venom of the Portuguese man-of-war, *Physalia physalis*. *Biochem. Biophys. Acta.* 667: 87–98.
- Thomas, C. & S. Scott, 1997. *All Stings Considered*. University of Hawaii Press, Honolulu. 231 pp.
- Totton, A.K. & G.O. Mackie, 1960. Studies on *Physalia physalis*. *Discovery Rep.* 30: 301–408.
- Watson, G.M., 1988. Ultrastructure and cytochemistry of developing nematocysts. In: Hessinger, D. A. & H. M. Lenhoff (Eds.), *The Biology of Nematocysts*. Academic Press, Inc., San Diego, pp. 143–164.
- Watson, G.M. & R.N. Mariscal, 1984. Calcium cytochemistry of nematocyst development in catch tentacles of the sea anemone *Haliplanella luciae* (Cnidaria: Anthozoa) and the molecular basis for tube inversion into the capsule. *J. Ultrastruct. Res.* 86: 202–214.
- Watson, G.M. & R.L. Wood, 1988. Colloquium on Terminology. In: Hessinger, D. A. & H. M. Lenhoff (Eds.), *The Biology of Nematocysts*. Academic Press, Inc., San Diego, pp. 21–23.
- Weber, J., 1991. A novel kind of polyanions as principal components of cnidarian nematocysts. *Comp. Biochem. Physiol.* 98A: 285–291.
- Weill, R., 1934. Contribution à l'étude des cnidaires et de leurs nématocystes: (2 vols.). *Trav. Sta. Zool. Wimereux I* 10: 1–347; *II* 11: 348–701.
- Williamson, J.A., P.J. Fenner & J.W. Burnett, 1996. Principles of patient care in marine envenomations and poisonings. In: Williamson, J. A., P. J. Fenner, J. W. Burnett, & J. F. Rifkin (Eds.), *Venomous and Poisonous Marine Animals: A Medical and Biological Handbook*. University of New South Wales Press, Sydney, pp. 98–117.
- Yanagita, T.M. & T. Wada, 1959. Physiological mechanism of nematocyst response in sea-anemone. VI. A note on the microscopical structure of acontium, with special reference to the situation of cnidae within its surface. *Cytologia (Tokyo)* 24: 81–97.
- Yanagihara, A.A., J.M.Y. Kuroiwa, L.M. Oliver, J.J. Chung & D.D. Kunkel, 2002. Ultrastructure of a novel eurytele nematocyst of *Carybdea alata* Reynaud (Cubozoa, Cnidaria). *Cell Tissue Res.* 308: 307–318.